NANO LETTERS

2009
Vol. 9, No. 11
3715-3719

Inhibiting Strain-Induced Surface Roughening: Dislocation-Free Ge/Si and Ge/SiGe Core−Shell Nanowires

Irene A. Goldthorpe,*,† Ann F. Marshall,‡ and Paul C. McIntyre†,‡

Materials Science and Engineering and Geballe Laboratory for Advanced Materials, Stanford University, Stanford, California 94305

Received June 8, 2009; Revised Manuscript Received September 3, 2009

ABSTRACT

Elastic strain is a critical factor in engineering the electronic behavior of core−shell semiconductor nanowires and provides the driving force for undesirable surface roughening and defect formation. We demonstrate two independent strategies, chlorine surface passivation and growth of nanowires with low-energy sidewall facets, to avoid strain-induced surface roughening that promotes dislocation nucleation in group IV core−shell nanowires. Metastably strained, dislocation-free, core−shell nanowires are obtained, and axial strains are measured and compared to elasticity model predictions.

Strain engineering and defect formation mechanisms in planar two-dimensional epitaxial heterostructures are long-standing topics of both fundamental and practical interest.[1−6] Recently, substantial attention has been focused on synthesizing coaxial nanowire heterostructures using lattice misfitting semiconductors.[7−14] Such structures can improve the performance of nanoelectronic devices by increasing conductivity through strain-induced mobility enhancements[15,16] and creating band offsets to spatially separate carriers from scattering centers such as surface states and ionized dopants.[17−19] In nanophotonic devices, confining carriers away from the surface can increase emission efficiency,[10] and the band gap can be tailored through strain effects[10,20] and quantum confinement.[21,22]

There are several reports of dislocation-free core−shell nanowires.[10,11,17,23] Maintaining coherency by purely elastic deformation is possible on thermodynamic grounds for low misfit core−shell materials systems.[11,24−27] However, core−shell nanowires are not, in general, sufficiently compliant to elastically accommodate large misfit strains,[24−27] such as the 4.2% lattice mismatch between pure Ge and pure Si, explaining the inelastic strain relaxation reported in many experiments.[8,9,12,14] The unexpected observation of coherent Ge-core/Si-shell nanowires reported in the literature[7,17] awaits an adequate explanation. Moreover, a general approach for achieving metastably coherent Ge-core/Si-shell nanowires has not been demonstrated. In this paper, we show that by inhibiting surface roughening of a Si or SiGe shell around a Ge nanowire, dislocation formation can be prevented and coherent structures are obtained.

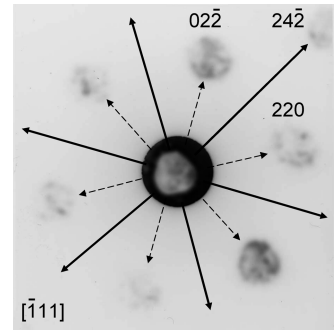

Figure 1. A convergent beam electron diffraction pattern showing the direct orientation relationship between the cross section of a ⟨111⟩-oriented germanium nanowire (shadow diffraction image in center) and its diffraction reflections. The dotted arrows point to the six {220} reflections and the solid arrows bisecting them point to the {224} reflections. The six facets of the nanowire are all {112} planes.

In our experiments, Ge nanowires were first grown by chemical vapor deposition through the vapor−liquid−solid (VLS) mechanism, as previously described.[28] Germane in a hydrogen carrier gas was used as the precursor and 10 or 40 nm colloidal gold nanoparticles were used as catalysts. Nanowires produced using the 40 nm catalysts are ⟨111⟩-oriented with six {112} side facets, as determined by transmission electron microscopy (TEM) (Figure 1). These nanowires were vertically aligned through epitaxial growth on Si(111) substrates. The lattice mismatch between Ge and Si is far greater than the theoretically predicted maximum mismatch a core−shell nanowire with a 40 nm core can

* Corresponding author, goldthorpe@stanford.edu.
† Materials Science and Engineering.
‡ Geballe Laboratory for Advanced Materials.

10.1021/nl9018148 CCC: $40.75 © 2009 American Chemical Society
Published on Web 10/01/2009

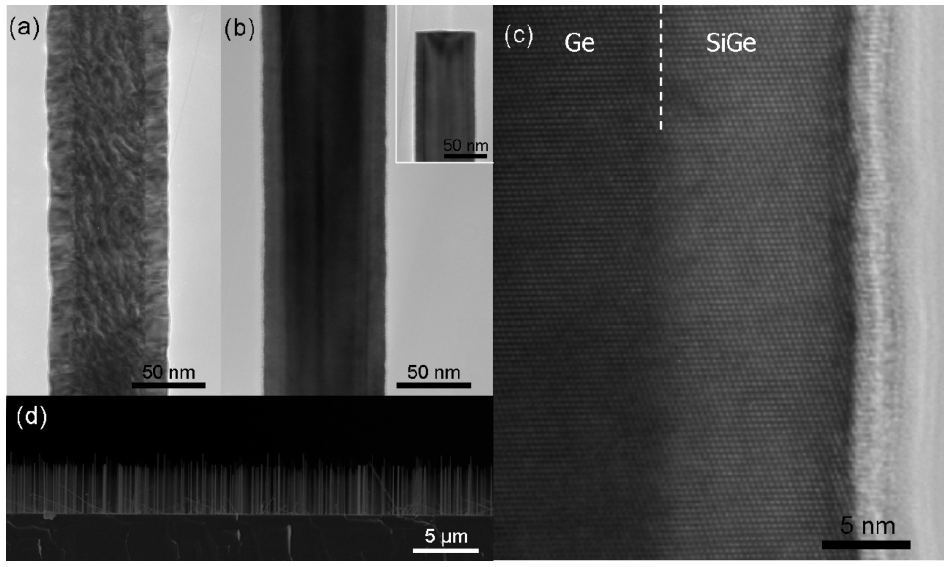

Figure 2. Using HCl to obtain dislocation-free Ge/$Si_{0.25}Ge_{0.75}$ core−shell nanowires. (a) TEM image of a SiGe shell deposited on a Ge nanowire without HCl. The shell has misfit dislocations. (b, c) TEM images of a core−shell nanowire in which the SiGe shell was deposited using the same conditions as in (a), but with the addition of gaseous HCl flowing at 10 sccm. Inset, tip of core−shell nanowire. (d) SEM image of vertically aligned dislocation-free Ge/SiGe core−shell nanowires.

coherently accommodate.[24−27] Therefore, in experiments on Ge nanowire cores grown using 40 nm catalysts, SiGe shells, rather than Si shells, were deposited conformally around the cores. SiGe was deposited at 585 °C at a total pressure of 25 Torr, with germane flowing at 2 sccm, silane at 7.5 sccm, and a hydrogen carrier gas at 818 sccm. At this temperature, some of the gold catalyst diffused into the nanowire. For applications where Au impurities need to be avoided, the gold should be etched selectively, as demonstrated previously.[8]

The core−shell nanowires were examined in a Philips CM-20 field-emission gun (FEG) TEM. The nanowires were not removed from the Si substrate; a thin piece of the sample was cut and mounted sideways in a TEM holder. It was observed that, similar to the case of pure Si deposition on Ge nanowires of this diameter,[8] the surface of the Ge-core/SiGe-shell nanowire (Figure 2a) roughened, and Moiré fringes and misfit dislocations in the shell indicated that the structure is at least partially relaxed.

Our previous study[8] demonstrated that roughening during growth of the misfitting Si shell around a Ge core precedes nucleation of dislocations which relieve most of the axial misfit strain in these structures. As is the case of planar heteroepitaxy in the Si−Ge system,[2,3] stress-driven roughening via surface diffusion on the epilayer produces regions of stress concentration in the misfitting shell at which dislocations appear to nucleate preferentially. Given the importance of adatom surface diffusion to the roughening kinetics, shell deposition in the presence of chemical species that compete for surface sites on the shell can inhibit surface roughening. It has been shown that the presence of chlorine surface atoms impedes adatom surface diffusion on planar Ge[29] and Si[30] substrates. Therefore, we performed deposition under the same deposition conditions as used for the sample in Figure 2a, but added HCl at a flow rate of 10 sccm (Figure 2b,c). The surface of the SiGe shell is smooth. Both low-magnification bright-field TEM images and high-resolution TEM images of hundreds of wires failed to detect any dislocations, stacking faults, twins, or grain boundaries in these structures.

The shell surface during conformal SiGe layer deposition is likely Si-rich. When a planar SiGe surface is exposed to HCl above ∼400 °C, Si atoms segregate to the surface so that the majority of surface species is Cl-terminated Si.[31] Much higher temperatures are required for chlorine to desorb from a Si surface compared to a Ge surface (∼630 °C for Si(100) compared to ∼350 °C for Ge(100)[32]). At 585 °C and for total pressure and HCl partial pressures similar to those used in our experiments, the reported etching rate of planar SiGe films is rather low (<1 nm/min).[33] Considering these previously reported results, we expect that chlorine atoms supplied by the decomposition of HCl passivates (at least transiently) dangling bonds on some of the surface atoms during shell deposition and that this slows adatom surface diffusion. Because adatom migration requires broken bonds on the nanowire sidewall surfaces, diffusion onto a site that is initially Cl terminated requires that a Si−Cl bond be broken. A deposition rate of 10 nm/min is sufficiently high for the adatoms to be buried before the surface has sufficient time to roughen; however, it was observed that when the deposition rate was increased above 15 nm/min by increasing the total pressure in the reactor, other defects, such as stacking faults and twins, formed. When the deposition rate was less than 7 nm/min, surface roughening occurred, presumably because of strain driven adatom surface diffusion.

In addition to the SiGe shell deposition rate, there is an optimal HCl flow rate. At HCl flow rates between 10 and 20 sccm, the shell has a rough surface. At still higher HCl flow rates (above 20 sccm), we observed that no SiGe is deposited at all. At these higher HCl flow rates, the Cl passivation may inhibit SiGe deposition. In addition, the shell

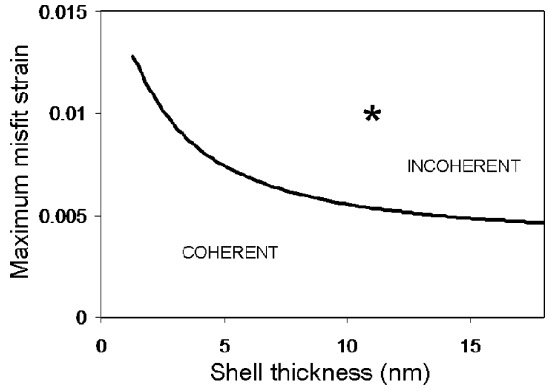

Figure 3. The critical misfit strain a core−shell nanowire with a 48 nm diameter core is predicted to be able to accommodate before dislocations form (adapted from ref 26). The star corresponds to the misfit strain and shell thickness of the dislocation-free 48 nm Ge core/12 nm $Si_{0.25}Ge_{0.75}$ shell nanowires shown in Figure 2b−d and indicates that coherent core−shell nanowires were synthesized with higher misfit strains than those predicted by equilibrium calculations.

surface may be etched at a rate comparable to the deposition rate. An approximately quadratic relationship between the etching rate of planar SiGe (100) surfaces with increasing HCl partial pressure has been reported.[33]

The Ge nanowire cores of the sample shown in Figure 2b−d have diameters of 48 ± 4 nm, and the shells are 12 ± 1 nm thick. Energy dispersive X-ray spectroscopy (EDS) determined the shells to be Si_xGe_{1-x} with $x = 0.25 \pm 0.04$. This corresponds to a 1% lattice mismatch between the core and shell. The plot in Figure 3, constructed using the continuum mechanics calculations of Liang et al.,[26] predicts the maximum magnitude of misfit strain between the core and shell that the structure can coherently accommodate before the formation of dislocations becomes energetically favorable. For a 48 nm core with a 12 nm shell, this maximum misfit strain is 0.52%. Their analysis, however, considers equilibrium conditions only and not kinetics. In the present case, by using HCl to inhibit surface roughening, local stress concentrations in the shell which facilitate nucleation of dislocations are avoided. This allows the synthesis of core−shell nanowires with higher misfit strains than the maximum values predicted by equilibrium calculations.

Selected area electron diffraction (SAED) patterns were collected on the $[\bar{1}\bar{1}2]$ zone axis of a 48 nm diameter Ge nanowire (Figure 4a) and a core−shell nanowire in the coherent core−shell wire array shown in Figure 2b−d (Figure 4b). The horizontal streaking of the peaks is a result of the small diameters of the nanowires. A single diffraction spot from the (111) Si and Ge planes is observed in Figure 4b, demonstrating that the spacing of the axial planes of the Ge core is equal to the spacing of the axial planes in the SiGe shell. This is consistent with the absence of misfit dislocations in the structure. The spot corresponding to the $(\bar{2}20)$ planes of the core−shell nanowire, which are perpendicular to the radius of the core and the shell, is not a single feature as it is for the single-component Ge nanowire in Figure 4a. Like the axial (111) reflection, this is again consistent with a coherently strained core−shell nanowire. The radial plane spacing throughout the radius of a coherently strained core−shell nanowire of the same dimensions, as predicted by continuum mechanics,[26] is plotted in Figure 4c. The radial Ge planes are compressed equally (compared to bulk Ge) throughout the nanowire core. The radial stress in the shell is also compressive, but decays in magnitude from a maximum value at the core/shell interface to zero at the shell surface, as required for mechanical equilibrium. The continuum mechanics calculations are consistent with the observation in Figure 4b of a single $(\bar{2}20)$ diffraction spot from the Ge core and a horizontally broadened spot shifted from that of the Ge core, corresponding to diffraction from $(\bar{2}20)$ planes in the coherent SiGe shell.

Vertically aligning the core−shell nanowires enables quantitative axial strain measurements by X-ray diffraction. Figure 4d displays symmetric diffraction data measured from the axial Ge(111) planes (perpendicular to the nanowire growth axis) for four different nanowire arrays. The interplanar spacing of 48 nm diameter Ge nanowires without shells exactly matched that of relaxed Ge, and thus the single-component Ge nanowires were unstrained. With coherent $Si_{0.25}Ge_{0.75}$ shells of 5.5 and 12 nm, the measured average axial strains of the Ge nanowire cores were −0.22% and −0.43%, respectively. The −0.43% strain in the 48 nm core/12 nm shell nanowires corresponds to an axial compressive stress of 6.1×10^8 Pa in the core. For unrelaxed core−shell nanowires, continuum mechanics predicts axial strains of −0.34% and −0.56% in 48 nm Ge nanowires with 5.5 and 12 nm $Si_{0.25}Ge_{0.75}$ shells, respectively. Thus the measured values are somewhat less than the predicted values. However, even though the volume of the cores and shells are similar (in the case of a 48 nm core/12 nm shell nanowire, the shell volume is 1.25 times that of the core volume), the existence of only one diffraction peak demonstrates, as does the SAED diffraction pattern in Figure 4b, that the axial plane spacings in the core and shell are equal to one another. Interdiffusion between the Ge core and SiGe shell or approximations made in the continuum mechanics analysis likely account for the modest quantitative discrepancy between the experimentally measured strains and the theoretically predicted values. Figure 4d also shows the diffraction peak from the sample shown in Figure 2a. The full width at half-maximum is greater than those of the other three peaks, and the strain was measured to be −0.27%. Thus, when no HCl flow is used during shell deposition, there is a broader spectrum of interplanar spacings and less strain in the nanowire as compared to when the shell is deposited in the presence of HCl. The diffraction data are therefore consistent with the observation of misfit dislocations in these core−shell nanowires by TEM.

In our previous study of Si shell deposition on Ge nanowires, we observed that stress-driven surface roughening caused the {112} sidewall facets of the as-grown Ge wires to break up into a hill-and-valley structure of lower-energy planes.[8] Therefore, in addition to using HCl to inhibit surface roughening, we also studied the possibility of avoiding surface roughening through the synthesis of core−shell

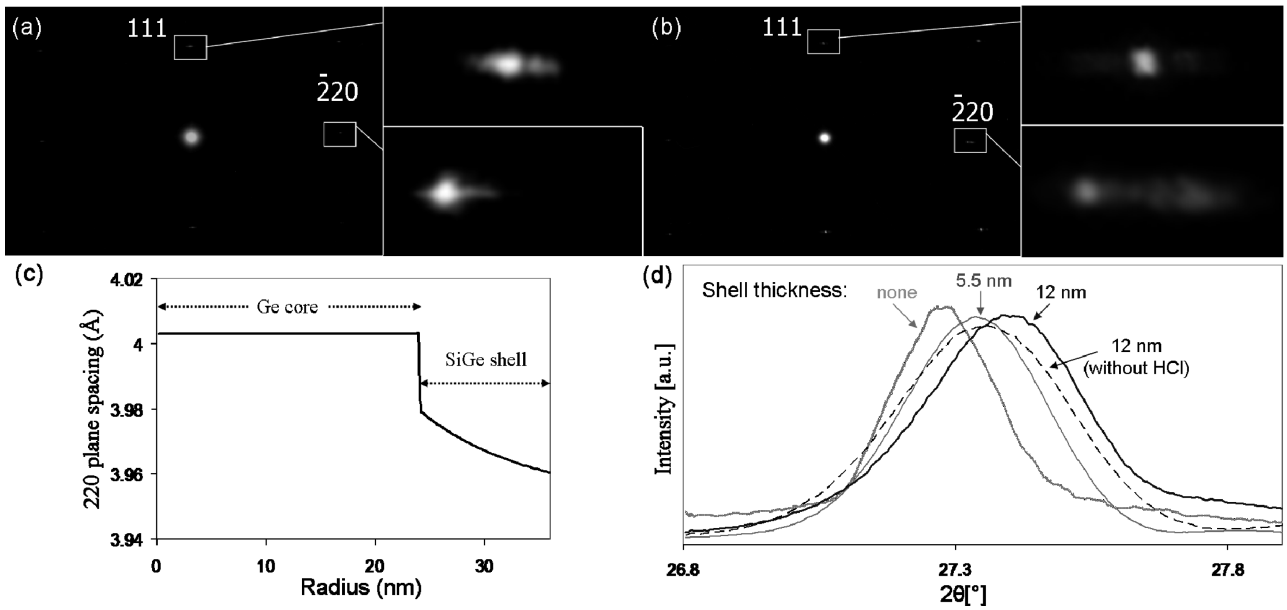

Figure 4. Core−shell nanowire strain characterization. Selected area diffraction pattern of (a) a 48 nm diameter germanium nanowire and (b) a core−shell nanowire of the sample shown in Figure 2b−d, indicating that the strain is accommodated coherently. (c) The predicted radial plane spacings throughout a coherent core−shell nanowire of the same dimensions as the wire characterized in (b). Plot is consistent with diffraction from (−220) planes in (b). (d) X-ray diffraction peaks indicating the axial plane spacings of 48 nm Ge nanowires without shells, with 5.5 and 12 nm $Si_{0.25}Ge_{0.75}$ shells deposited in the presence of HCl, and with 12 nm $Si_{0.25}Ge_{0.75}$ shells deposited without HCl.

nanowires of another crystallographic orientation, bounded by surfaces facets that are more stable than {112} planes. This approach exploits the energetic cost of roughening from low energy planes toward planes with higher surface energies, with a simultaneous increase in total surface area, so as to inhibit strain-energy-reducing roughening processes. Nanowires with low-energy surface facets were obtained by growing Ge nanowires with diameters smaller than 20 nm, as these nanowires are predominantly ⟨110⟩-oriented, with four {111} and two {100} side facets.[34] The {111} and {100} planes are the two most stable surfaces of Si.[35] Ge nanowires with ⟨110⟩ growth axes were grown epitaxially on Ge(110) substrates using 10 nm gold nanoparticles as catalysts. The resulting Ge nanowires had diameters of 13 ± 2 nm.

When Si is deposited on nanowires with {112} surface facets, even the thinnest shells have a tendency to roughen.[8] It is possible to deposit thin dislocation-free shells on these nanowires, but the shell surface develops periodic undulations at the temperatures required for Si heteroepitaxy. In contrast, when Si was deposited on the ⟨110⟩-oriented Ge nanowires, the surface did not roughen significantly. Shells of 1.8 nm thicknesses were deposited around Ge nanowires at 700 °C and 10 Torr total pressure, with a silane flow of 7.5 sccm, HCl flow of 6.5 sccm, and a hydrogen carrier gas flow of 300 sccm (Figure 5). The resulting surface is relatively smooth. Continuum elasticity calculations predict that dislocations should exist in these core−shell nanowires;[26] however, no dislocations were detected in TEM analysis of hundreds of core−shell nanowires. HCl gas was used to slow the effective Si deposition rate from 8 nm/min to 3 nm/min, but its presence is not necessary to maintain a smooth surface, as the surface did not roughen when shells were deposited without HCl. Avoiding roughening and thus kinetically

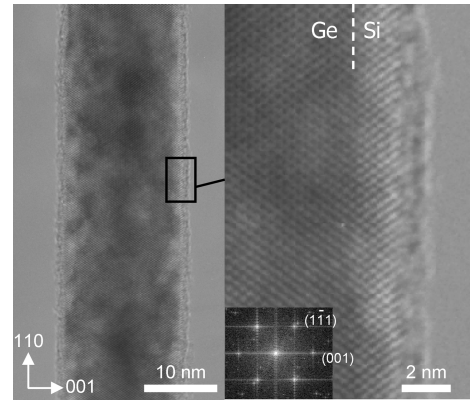

Figure 5. TEM image of a dislocation-free Ge-core/Si-shell nanowire. Because ⟨110⟩-oriented Ge nanowires have low-energy side facets, Si shell roughening is inhibited, allowing relatively smooth, dislocation-free shells less than 2 nm in thickness to be deposited. Inset: two-dimensional Fourier transform of the real-space image, confirming the ⟨110⟩ growth direction of the nanowire.

inhibiting dislocation formation by synthesizing nanowires with surface facets that are more stable than {112} facets, as well as using small diameter cores (<15 nm) which are more elastically compliant than larger wires, may explain why Lu et al.[17] were able to directly deposit smooth, dislocation-free, thin Si shells around Ge nanowires. Their nanowires had a ⟨112⟩ growth orientation, which others have reported are bounded by surfaces of low energy.[9] In another report, Lauhon et al.[7] deposited amorphous Si shells on Ge nanowires in the presence of diborane, which may have had a similar effect as chlorine passivation when the Si shell was subsequently crystallized through annealing. Boron is known to preferentially segregate to a Si(111) surface[36] and modify

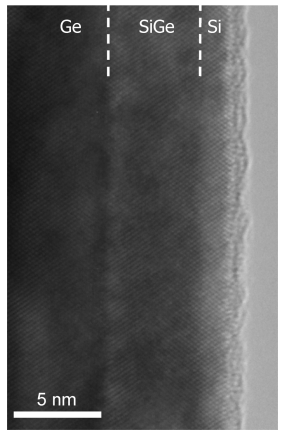

Figure 6. TEM image of a ⟨110⟩-oriented Ge/$Si_{0.25}Ge_{0.75}$/Si multishell nanowire.

its chemical properties by inducing a surface reconstruction without dangling bonds.[37]

When a Si shell thicker than ∼2 nm is deposited onto the ⟨110⟩-oriented Ge nanowires grown from 10 nm gold nanoparticles, dislocations are observed in the shell (see Supporting Information). The elastic strain is evidently high enough in these structures such that misfit dislocations can even nucleate beneath a smooth shell surface. For some applications, a dislocation-free shell thicker than 2 nm may be required on a ⟨110⟩- or ⟨112⟩-oriented nanowire. Depositing a SiGe shell, rather than a Si shell, allows a thicker dislocation-free shell to be deposited. In some instances, it may be desirable for the outer surface of a core−shell nanowire to be pure Si (e.g., to allow for a high-quality SiO_2 surface passivation to be grown on the shell surface). In such cases, a thin dislocation-free Si shell can be deposited around the SiGe shell (Figure 6). A similar approach—depositing multiple shells or a graded SiGe shell—could be used to obtain a Si surface on the larger ⟨111⟩-oriented nanowires. This reduces the effective misfit between the graded or composite core and the outermost Si shell, thus reducing the driving force for misfit dislocations to nucleate.

In conclusion, dislocation-free core−shell nanowires were synthesized with two different crystallographic VLS growth axes for the Ge cores. Germanium nanowires of 48 nm diameter were ⟨111⟩-oriented with {112} side facets. Inhibiting strain-induced roughening by depositing a SiGe shell in the presence of HCl avoids dislocation nucleation, allowing the synthesis of core−shell nanowires with a higher misfit strain than the critical value for dislocation formation as predicted by equilibrium calculations. Germanium nanowires of 13 nm diameter were predominantly ⟨110⟩-oriented, with {111} and {100} side facets which have lower energy compared to the {112} facet planes of the larger-diameter wires. Shells deposited on these nanowires did not roughen, allowing the synthesis of core−shell nanowires with thin, smooth, dislocation-free Si shells.

Acknowledgment. We thank the Agilent Foundation for financial support. I.A.G. acknowledges financial support from the David and Janet Chyan Stanford Graduate Fellowship and an Intel Ph.D. fellowship.

Supporting Information Available: TEM images showing dislocations in the shell of 110-oriented core-shell nanowires. This material is available free of charge via the Internet at http://pubs.acs.org.

References

(1) Matthews, J. W.; Blakeslee, E. *J. Cryst. Growth* **1974**, *27*, 118.
(2) Gao, H.; Nix, W. D. *Annu. Rev. Mater. Sci.* **1999**, *29*, 173.
(3) Ozkan, C. S.; Nix, W. D.; Gao, H. *Appl. Phys. Lett.* **1997**, *70*, 2247.
(4) van der Merwe, J. H. *Crit. Rev. Solid State Mater. Sci.* **1991**, *17*, 187.
(5) Mooney, P. M. *Mat. Sci. Eng. R* **1996**, *17*, 105.
(6) Hull, R.; Bean, J. C. *J. Vac. Sci. Technol., A* **1989**, *7*, 2580.
(7) Lauhon, L. J.; Gudiksen, M. S.; Wang, D.; Lieber, C. M. *Nature* **2002**, *420*, 57.
(8) Goldthorpe, I. A.; Marshall, A. F.; McIntyre, P. C. *Nano Lett.* **2008**, *8*, 4081.
(9) Pan, L.; Lew, K. K.; Redwing, J. M.; Dickey, E. C. *Nano Lett.* **2005**, *5*, 1081.
(10) Sköld, N.; Karlsson, L. S.; Larsson, M. W.; Pistol, M.-E.; Seifert, W.; Trägårdg, J.; Samuelson, L. *Nano Lett.* **2005**, *5*, 1943.
(11) Tambe, M. J.; Lim, S. K.; Smith, M. J.; Allard, L. F.; Gradečak, S. *Appl. Phys. Lett.* **2008**, *93*, 151917.
(12) Lin, H.-M.; Chen, Y.-L.; Yang, J.; Liu, Y.-C.; Yin, K.-M.; Kai, J.-J.; Chen, F.-R.; Chen, L.-C.; Chen, Y.-F.; Chen, C.-C *Nano Lett.* **2003**, *3*, 537.
(13) Schmidt, V.; McIntyre, P. C.; Gösele, U. *Phys. Rev B* **2008**, *77*, 235302.
(14) Keplinger, M.; Mårtensson, T.; Stangl, J.; Wintersberger, E.; Mandl, B.; Kriegner, D.; Holy, V.; Bauer, G.; Deppert, K.; Samuelson, L. *Nano Lett.* **2009**, *9*, 1877.
(15) He, R.; Yang, P. *Nat. Nanotechnol.* **2006**, *1*, 42.
(16) Lee, M. L.; Fitzgerald, E. A.; Bulsara, M. T.; Currie, M. T.; Lochtefeld, A. *J. Appl. Phys.* **2005**, *97*, 011101.
(17) Lu, W.; Xiang, J.; Timko, B. P.; Wu, Y.; Lieber, C. M. *Proc. Natl. Acad. Sci. U.S.A.* **2005**, *102*, 10046.
(18) Xiang, J.; Lu, W.; Hu, Y.; Yan, H.; Lieber, C. M. *Nature* **2006**, *441*, 489.
(19) Verdonckt-Vandebroek, S.; Crabbe, E. F.; Meyson, B. S.; Harame, D. L.; Restle, P. J.; Stork, J. M. C.; Megdanis, A. C.; Stanis, C. L.; Bright, A. A.; Kroesen, G. M. W.; Warren, A. C. *IEEE Electron Device Lett.* **1991**, *12*, 447.
(20) Lyons, D. M.; Ryan, K. M.; Morris, M. A.; Holmes, J. D. *Nano Lett.* **2002**, *2*, 811.
(21) Guichard, A. R.; Barsic, D. N.; Sharma, S.; Kamins, T. I.; Brongersma, M. L. *Nano Lett.* **2006**, *6*, 2140.
(22) Gudiksen, M. S.; Wang, J.; Lieber, C. M. *J. Phys. Chem. B* **2002**, *106*, 4036.
(23) Qian, F.; Li, Y.; Gradečak, S.; Wang, D.; Barrelet, C. J.; Lieber, C. M. *Nano Lett.* **2004**, *4*, 1975.
(24) Kolesnikova, A. L.; Romanov, A. E. *Philos. Mag.* **2004**, *84*, 501.
(25) Gutkin, M. Y.; Ovid'ko, I. A.; Scheinerman, A. G. *J. Phys.: Condens. Matter* **2000**, *12*, 5391.
(26) Liang, Y.; Nix, W. D.; Griffin, P. B.; Plummer, J. D. *J. Appl. Phys.* **2005**, *97*, 043519.
(27) Ovid'ko, I. A.; Sheinerman, A. G. *Philos. Mag.* **2004**, *84*, 2103.
(28) Woodruff, J. H.; Ratchford, J. B.; Goldthorpe, I. A.; McIntyre, P. C.; Chidsey, C. E. D. *Nano Lett.* **2007**, *7*, 1637.
(29) Kamins, T. I.; Briggs, G. A. D.; Williams, R. S. *Appl. Phys. Lett.* **1998**, *73*, 1862.
(30) Feil, H.; Dieleman, J.; Garrison, B. J. *J. Appl. Phys.* **1993**, *74*, 1303.
(31) Wu, M.-W.; Pan, S.-Y.; Hung, W.-H.; Lin, D.-S. *Surf. Sci.* **2002**, *507−510*, 295.
(32) Wu, J.-H.; Pan, S.-Y.; Lin, D.-S. *Phys. Rev. B* **2004**, *69*, 045308.
(33) Bogumilowicz, Y.; Hartmann, J. M.; Truche, R.; Campidelli, Y; Rolland, G.; Billon, T. *Semicond. Sci. Technol.* **2005**, *20*, 127.
(34) Ma, D. D. D.; Lee, C. S.; Au, F. C. K.; Tong, S. Y.; Lee, S. T. *Science* **2003**, *99*, 1874.
(35) Eaglesham, D. J.; White, A. E.; Feldman, L. C.; Moriya, N.; Jacobson, D. C. *Phys. Rev. Lett.* **1993**, *70*, 1643.
(36) Korobtsov, V. V.; Lifshits, V. G.; Zotov, A. V. *Surf. Sci.* **1988**, *195*, 466.
(37) Lyo, I.-W.; Kaxiras, E.; Avouris, P. *Phys. Rev. Lett.* **1989**, *63*, 1261.

NL9018148